

# Journal of Visualized Experiments

## Developing photosensitizer-Cobaloxime hybrid for solar-driven H<sub>2</sub> production in aqueous aerobic conditions --Manuscript Draft--

<b>Article Type:</b>	Invited Methods Article - Author Produced Video
<b>Manuscript Number:</b>	JoVE60231R2
<b>Full Title:</b>	Developing photosensitizer-Cobaloxime hybrid for solar-driven H <sub>2</sub> production in aqueous aerobic conditions
<b>Section/Category:</b>	JoVE Chemistry
<b>Keywords:</b>	Photocatalytic H <sub>2</sub> production, Cobaloxime, stilbene, photosensitizer-catalyst hybrid, online H <sub>2</sub> detection, artificial photosynthesis
<b>Corresponding Author:</b>	ARNAB DUTTA IIT Gandhinagar GANDHINAGAR, GUJARAT INDIA
<b>Corresponding Author's Institution:</b>	IIT Gandhinagar
<b>Corresponding Author E-Mail:</b>	Arnab.Dutta@iitgn.ac.in
<b>Order of Authors:</b>	ARNAB DUTTA Ab Qayoom Mir Dependu Dolui Shikha Khandelwal Harshil Bhatt Beena Kumari Sanmitra Barman Sriram Kanvah
<b>Additional Information:</b>	
<b>Question</b>	<b>Response</b>
Please indicate whether this article will be Standard Access or Open Access.	Standard Access (US\$1200)

**TITLE:**

**Developing Photosensitizer-Cobaloxime Hybrids for Solar-Driven H<sub>2</sub> Production in Aqueous Aerobic Conditions**

**AUTHORS AND AFFILIATIONS:**

Ab Qayoom Mir<sup>1</sup>, Dependu Dolui<sup>1</sup>, Shikha Khandelwal<sup>1</sup>, Harshil Bhatt<sup>2</sup>, Beena Kumari<sup>1</sup>, Sanmitra Barman<sup>3</sup>, Sriram Kanvah<sup>1</sup>, Arnab Dutta<sup>1</sup>

<sup>1</sup>Chemistry Discipline, Indian Institute of Technology Gandhinagar, Gujarat, India

<sup>2</sup>Chemistry Department, Uka Tarsadia University, Bardoli, Gujarat, India

<sup>3</sup>Applied Sciences Department, BML Munjal University, Haryana, India

Corresponding author:

Arnab Dutta

[arnab.dutta@iitgn.ac.in](mailto:arnab.dutta@iitgn.ac.in)

Email addresses of co-authors:

Ab Qayoom Mir ([ab.qayoom@iitgn.ac.in](mailto:ab.qayoom@iitgn.ac.in))

Dependu Dolui ([dependu.dolui@iitgn.ac.in](mailto:dependu.dolui@iitgn.ac.in))

Shikha Khandelwal ([shikha.khandelwal@iitgn.ac.in](mailto:shikha.khandelwal@iitgn.ac.in))

Harshil Bhatt ([harshilbhatt08@gmail.com](mailto:harshilbhatt08@gmail.com))

Beena Kumari ([kum.beena@iitgn.ac.in](mailto:kum.beena@iitgn.ac.in))

Sanmitra Barman ([sanmitra.barman@bmu.edu.in](mailto:sanmitra.barman@bmu.edu.in))

Sriram Kanvah ([sriram@iitgn.ac.in](mailto:sriram@iitgn.ac.in))

**KEYWORDS:**

Photocatalytic H<sub>2</sub> production, cobaloxime, stilbene, photosensitizer-catalyst hybrid, online H<sub>2</sub> detection, artificial photosynthesis.

**SUMMARY:**

We have directly incorporated a stilbene-based organic dye into a cobaloxime core to generate a photosensitizer-catalyst dyad for photocatalytic H<sub>2</sub> production. We have also developed a simple experimental setup for evaluating the light-driven H<sub>2</sub> production by photocatalytic assemblies.

**ABSTRACT:**

Developing photocatalytic H<sub>2</sub> production devices is the one of the key steps for constructing a global H<sub>2</sub>-based renewable energy infrastructure. A number of photoactive assemblies have emerged where a photosensitizer and cobaloxime-based H<sub>2</sub> production catalysts work in tandem to convert light energy into the H-H chemical bonds. However, the long-term instability of these assemblies and the need for hazardous proton sources have limited their usage. Here, in this work, we have integrated a stilbene-based organic dye into the periphery of a cobaloxime core via a distinct axial pyridine linkage. This strategy allowed us to develop a photosensitizer-catalyst hybrid structure with the same molecular framework. In this article, we have explained the

detailed procedure of the synthesis of this hybrid molecule in addition to its comprehensive chemical characterization. The structural and optical studies have exhibited an intense electronic interaction between the cobaloxime core and the organic photosensitizer. The cobaloxime was active for H<sub>2</sub> production even in the presence of water as the proton source. Here, we have developed a simple airtight system connected with an online H<sub>2</sub> detector for the investigation of the photocatalytic activity by this hybrid complex. This photosensitizer-catalyst dyad present in the experimental setup continuously produced H<sub>2</sub> once it was exposed in the natural sunlight. This photocatalytic H<sub>2</sub> production by the hybrid complex was observed in aqueous/organic mixture media in the presence of a sacrificial electron donor under complete aerobic conditions. Thus, this photocatalysis measurement system along with the photosensitizer-catalyst dyad provide valuable insight for the development of next generation photocatalytic H<sub>2</sub> production devices.

## INTRODUCTION:

In the modern world, fossil fuels such as coal, oil, and natural gas supply a majority share of the energy. However, they produce copious amount of CO<sub>2</sub> during the energy harvesting to negatively impact the global climate<sup>1</sup>. In coming years, a steep rise in energy demand is predicted worldwide following the continuous growth of population and constant improvement in human lifestyle. Thus, there is an active search for a suitable alternative energy resource to match the global energy requirement. Renewable energy resources like solar, wind, and tidal power have emerged as one of the best solutions due to their environment-friendly zero carbon energy transduction process<sup>2</sup>. However, the intermittent nature of these energy resources has so far limited their extensive application. A possible solution of this problem can be found in biology; solar energy is efficiently transformed into chemical energy during photosynthesis<sup>3</sup>. Following this clue, researchers have developed artificial photosynthetic strategies for storing solar energy into chemical bonds following a number of small molecule activation reactions<sup>4,5</sup>. The H<sub>2</sub> molecule has been considered one of the most appealing chemical vectors due to their high energy density and simplicity of their chemical transformation<sup>6,7</sup>.

The presence of a photosensitizer and a H<sub>2</sub> production catalyst are essential for an active solar-driven H<sub>2</sub> production setup. Here in this work, we will focus on the cobalt-based molecular complex cobaloxime for the catalytic segment. Typically, a hexa-coordinated cobalt center is bound in a square planar N<sub>4</sub> geometry, derived from the dimethylglyoxime (dmg) ligands, in cobaloximes. The complementary Cl<sup>-</sup> ions, solvent molecules (such as water or acetonitrile) or pyridine derivatives ligate in the residual axial positions<sup>8</sup>. Cobaloximes are long known for active H<sub>2</sub> production electrocatalysis and their reactivity can be tuned by appending variable functionalities on the axial pyridine<sup>9-12</sup>. The relatively uncomplicated syntheses, oxygen tolerance under catalytic conditions, and moderate catalytic response of cobaloximes have prompted researchers to explore their photocatalytic H<sub>2</sub> production reactivity. The Hawecker group was the pioneer in demonstrating the light-driven H<sub>2</sub> production activity of cobaloximes by utilizing Ru(polypyridyl)-based photosensitizers<sup>13</sup>. Eisenberg and his coworkers utilized platinum (Pt)-based inorganic photosensitizers to induce photocatalytic H<sub>2</sub> production in tandem with cobaloxime catalysts<sup>14,15</sup>. Later, the Che group utilized organo-gold photosensitizer to replicate similar activity<sup>16</sup>. Fontecave and Artero expanded the range of photosensitizers by

applying iridium (Ir)-based molecules<sup>17</sup>. The practical applications of these photocatalytic systems were heading towards a roadblock due to the use of expensive metal-based photosensitizers. The Eisenberg and Sun research groups have countered that by independently devising organic dye-based photo-driven H<sub>2</sub> production systems<sup>18,19</sup>. Despite the successful photo-driven H<sub>2</sub> production by all these systems, it was observed that the overall catalytic turnovers were relatively slow<sup>20</sup>. In all these cases, the photosensitizer and cobaloxime molecules were added as separate moieties in the solution, and the lack of direct communication between them might have hindered the overall efficiency of the system. A number of photosensitizer-cobaloxime dyads were developed to rectify this issue, where a variety of photosensitizers were directly linked with the cobaloxime core via the axial pyridine ligand<sup>21–26</sup>. Sun and co-workers were even successful in developing a noble-metal free device by introducing a Zn-porphyrin motif as a photosensitizer<sup>24</sup>. Recently, Ott and coworkers have successfully incorporated the cobaloxime catalyst within an metal organic framework (MOF) that displayed photocatalytic H<sub>2</sub> production in the presence of organic dye<sup>27</sup>. However, the inclusion of the high molecular weight photosensitizers into the cobaloxime framework reduced the water solubility while affecting the long-term stability of the dyads under catalytic conditions. The stability of the active dyads under aqueous conditions during the catalysis is crucial as the omnipresent water is an attractive source of protons during the catalysis. Thus, there is a serious need for developing an aqueous soluble, air-stable photosensitizer-cobaloxime dyad system to establish an efficient and economical photo-driven H<sub>2</sub> production setup.

Here in this work, we have anchored a stilbene-based organic dye<sup>28</sup> as photosensitizer to the cobaloxime core via the axial pyridine linker (**Figure 1**). The light molecular weight of the dye ensured improved water solubility of the dyad. This stilbene-cobaloxime hybrid molecule was characterized in detail via optical and <sup>1</sup>H NMR spectroscopy along with its single crystal structure elucidation. The electrochemical data revealed the active electrocatalytic H<sub>2</sub> production by the cobaloxime motif even with the appended organic dye. This hybrid complex exhibited significant photo-driven H<sub>2</sub> production when exposed to direct sunlight in the presence of an appropriate sacrificial electron donor in a 30:70 water/DMF (N,N'-dimethylformamide) solution without any degradation of the hybrid structure as complemented by optical spectroscopy studies. A simple photocatalytic device, consisting of a H<sub>2</sub> detector, was employed during the photocatalysis of the hybrid complex that demonstrated continuous production of H<sub>2</sub> gas under aqueous aerobic condition without any preliminary lag period. Thus, this hybrid complex has the potential to become the base for developing the next generation of solar-driven H<sub>2</sub> production catalysts for efficient renewable energy utilization.

## PROTOCOL

### 1. Synthesis of the photosensitizer-catalyst hybrid

#### 1.1. Synthesis of catalyst precursor Co(dmg)<sub>2</sub>Cl<sub>2</sub> complex

NOTE: This complex was synthesized following the modified version of the reported procedure<sup>29</sup>.



1.1.1. Dissolve 232 mg (1 mmol) of dimethylglyoxime (dmg) ligand (two equivalents in this reaction) in 27 mL of acetone.

1.1.2. Dissolve 118 mg (0.5 mmol) of  $\text{CoCl}_2 \cdot 6\text{H}_2\text{O}$  (one equivalent in this reaction) in 3 mL of deionized water separately that produces a pink color solution.

1.1.3. Add the aqueous  $\text{CoCl}_2$  solution drop wise to the acetone solution containing dmgl with continuous stirring at room temperature.

1.1.4. Closely monitor the change in the solution color, which will sequentially turn to bluish green color following the metal addition.

1.1.5. Continue the reaction for 2 h.

1.1.6. Filter the reaction mixture through a Grade 40 filter paper and keep the filtrate at 4 °C overnight.

1.1.7. The next day, obtain the green colored precipitate of  $\text{Co}(\text{dmgl})_2\text{Cl}_2$  complex (cobaloxime) from the solution and filter it through grade 40 filter paper.

1.1.8. Dry the sample under air.

## **1.2. Synthesis of the photosensitizer (PS)-cobaloxime hybrid**

NOTE: The stilbene based photosensitizer (PS) was synthesized as per the reported method<sup>28</sup>. The following steps were followed for the PS-catalyst hybrid complex synthesis.

1.2.1. Add 100 mg (0.277 mmol) of cobaloxime (one equivalent) (synthesized in Step 1) in 5 mL of methanol. It will form a green suspension.

1.2.2. Add 38  $\mu\text{L}$  (0.277 mmol) of triethylamine (TEA) base (one equivalent) to the green suspension with continuous stirring. The solution will turn transparent brown after within 1 min.

1.2.3. Add 65 mg (0.277 mmol) of solid stilbene dye (one equivalent) to the previously mentioned TEA added cobalt solution in methanol.

1.2.4. Continue the stirring for 3 h. Closely monitor the change in the solution, which will sequentially produce the reddish-brown precipitate of the PS-cobaloxime hybrid.

1.2.5. Filter the reddish-brown precipitate with Grade 40 filter paper and wash it with copious amount of cold methanol (20 mL).

1.2.6. Dissolve the precipitate in chloroform (10 mL) and collect the reddish-brown filtrate.

1.2.7. Evaporate the filtrate under reduced pressure using a rotavapor at room temperature.

1.2.8. Collect the solid reddish-brown product [Observed yield: 76 mg (65%)].

1.2.9. Recrystallize the product from chloroform solution at room temperature, where the chloroform evaporates slowly to produce reddish-brown crystals of the complex.

## **2. Characterization of the photosensitizer-cobaloxime hybrid**

### **2.1. NMR characterization**

2.1.1. Dissolve 5.0 mg of the purified PS-Cobaloxime hybrid complex in 650  $\mu\text{L}$  of  $d^6$ -DMSO.

2.1.2. Record the  $^1\text{H}$  NMR in NMR spectrometer at room temperature.

NOTE:  $^1\text{H}$  NMR signals, in  $\delta$  (ppm) units with the corresponding number of protons, their identity, and the splitting pattern in parentheses (s = singlet, d = doublet, m = multiplet), are as following:  
 $^1\text{H}$  NMR: 2.34 (12H, -dmg- $\text{CH}_3$ , s), 2.97 (6H, -dye-N-( $\text{CH}_3$ ) $_2$ , s), 6.74 (2H, dye-aromatic, d), 6.84 (1H, allylic-H, d), 7.48 (5H, four dye-aromatic, one allylic-H, m), 7.82 (2H, dye-aromatic, d), 18.47 (2H, dmg-NOH, s).

### **2.2. UV-Vis spectroscopy**

2.2.1. Prepare a 1.0 mM solution of the PS-cobaloxime complex in N,N'-dimethylformamide (DMF) by adding the appropriately weighed amount of the complex in the solvent.

2.2.2. Dilute the solution 10 times with blank DMF to generate 0.1 mM solution of the hybrid complex in DMF.

2.2.3. Further dilute it 5 times with blank DMF to generate 20  $\mu\text{M}$  solution of the hybrid complex in DMF.

2.2.4. Record the optical spectra of the 20  $\mu\text{M}$  PS-cobaloxime complex solution using a spectrophotometer.

NOTE: UV-Vis peaks ( $\lambda/\text{nm}$ ), with the corresponding molar extinction coefficient ( $\epsilon / \text{M}^{-1}\text{cm}^{-1}$ ) in parentheses, are as follows: 266 (13400) and 425 (14600).

### **2.3. Single crystal structure determination**

2.3.1. Prepare a concentrated 0.2 M sample of the PS-catalyst hybrid complex in 5 mL of chloroform. Grow reddish-brown (cubic) crystals of the complex from that chloroform solution over 3 days.

2.3.2. Select a suitable crystal of the complex and mount on a cryo-loop using cryoprotectant (e.g., Paratone oil).

2.3.3. Collect the single crystal diffraction data for the hybrid complex at 298 K on the diffractometer.

2.3.4. Apply the empirical absorption correction to the data by employing the multi-scan method in SADABS programming<sup>30</sup>.

2.3.5. Resolve the structure by direct methods with SHELXS-97 and refine by the full matrix least square methods on  $F^2$  using the SHELXL-2014<sup>31</sup>.

## **2.4. Electrochemical studies**

### **2.4.1. Sample preparation**

2.4.1.1. Prepare a 1 mM solution of the PS-catalyst hybrid complex in HPLC grade DMF containing 0.1 M tetra-N-butyl ammonium fluoride ( $n\text{-Bu}_4\text{N}^+\text{F}^-/\text{TBAF}$ ).

2.4.1.2. Place 2 mL of the sample solution prepared in step 1 in the electrochemical cell (volume 5 mL).

2.4.1.3. Purge  $\text{N}_2$  gas through the solution for 30 min to remove oxygen.

### **2.4.2. Electrode preparation**

2.4.2.1. Polish the 1 mm diameter glassy carbon-disc working electrode with 0.25  $\mu\text{m}$  alumina paste prepared in water on a polishing pad.

2.4.2.2. Rinse the polished electrode thoroughly with a copious amount of deionized water.

2.4.2.3. Place the clean working electrode in the electrochemical cell.

2.4.2.4. Place the Ag/AgCl (in 1.0 M  $\text{AgNO}_3$ ) reference electrode and the platinum (Pt)-wire counter electrode in the electrochemical cell.

2.4.2.5. Connect all the electrodes accordingly to the potentiostat.

### **2.4.3. Collecting data**

2.4.3.1. Stop the  $\text{N}_2$  gas purging before the electrochemical experiment.

2.4.3.2. Keep a continuous flow of  $\text{N}_2$  above the sample solution in the electrochemical cell.

2.4.3.3. Record cyclic voltammograms (CV) of the sample starting from the anodic direction to cathodic direction with appropriate scan rate (0.1 V/s scan rate was used in this experiment).

2.4.3.4. Repeat the above experiment by adding appropriate amounts of water (30% water in DMF) and trifluoroacetic acid (TFA) (8  $\mu$ L of 10x diluted neat TFA), respectively.

2.4.3.5. Add ferrocene to the sample solution and record the corresponding CV. Adjust the potential scale with the ferrocene couple ( $\text{FcCp}_2^{+/0} = 0\text{V}$  vs. Ferrocene) for all the collected data. Thus, all the potential values mentioned in this work was internally referenced against Ferrocene couple.

### **3. Catalytic H<sub>2</sub> production by the photosensitizer-catalyst hybrid in sunlight**

#### **3.1. Photocatalytic H<sub>2</sub> production by the PS-catalyst hybrid complex**

3.1.1. Prepare 0.2 mM PS-catalyst hybrid complex in 10 mL of 70:30 DMF water (pH 7, 0.1 MES buffer) in a two-neck test tube.

3.1.2. Add 1 mL of triethanolamine (TEOA) as the sacrificial electron donor to the sample solution.

3.1.3. Close the two openings of the test tube with the air-tight septum.

3.1.4. Connect this setup with the H<sub>2</sub> detector with appropriate tubing connections.

NOTE: The H<sub>2</sub> detector has two tube connections. One of them acts as the input that goes through an in-built detector to measure the amount of H<sub>2</sub> (in ppm units) present in the sample. The measured gas sample then connects back to the reaction vessel by the output tubing.

3.1.5. Place the set up under sunlight for 30 min and monitor the H<sub>2</sub> production rate via the detector.

#### **3.2. Monitoring the solar-driven H<sub>2</sub> production via gas chromatography (GC)**

3.2.1. Collect 1 mL of headspace gas via gas-tight syringe.

3.2.2. Inject the collected gas in the gas chromatography (GC) instrument.

3.2.3. Monitor the resulted gas chromatograph.

3.2.4. Inject 1 mL of headspace gas collected from a control sample placed under dark.

3.2.5. Inject 1 mL of gas from a calibrated standard gas mixture containing 1% H<sub>2</sub>.

## REPRESENTATIVE RESULTS:

In this work, a stilbene photosensitizer-cobaloxime hybrid complex (**C1**) was synthesized successfully by anchoring the organic dye (**L1**) derived pyridine motif as the axial ligand to the cobalt core. The  $^1\text{H}$  NMR data of the hybrid complex clearly demonstrated the presence of both the cobaloxime and organic dye protons in the same complex. As shown in **Figure 2**, the up-fielded aliphatic region highlighted the presence of both oxime-bound methyl and stilbene N-dimethyl proton signals in appropriate proportions at  $\delta$  (ppm) 2.34 and 2.97, respectively. The aromatic and unique allylic proton signals from the stilbene skeleton were sighted in the 6.74-7.82  $\delta$  (ppm) region, which was highlighted in detail in the inset of **Figure 2**. The stability of the cobaloxime core was exemplified by the presence of the intra-molecular hydrogen bonding in the oxime moiety in the far down field region ( $\sim 12.47$   $\delta$  (ppm))<sup>11</sup>. The optical spectra of the hybrid complex **C1** exhibited two major signals (**Figure 3**). In the UV region, a distinct signal was observed at 266 nm. This signal resembled the characteristic  $\pi-\pi^*$  transition originated from the oxime scaffold. Another optical transition was noticed for **C1** in the visible region at 425 nm. This signal is significantly red-shifted compared to the typical  $\pi-\pi^*$  transition observed for the stilbene compound ( $\lambda_{\text{max}}$  385 nm) (**Figure 3**)<sup>32</sup>. This transition observed in **C1** possibly has significant contribution from the  $\text{N}^{\text{pyridine}}\text{-Co(III)}$  ligand to metal charge transfer (LMCT) transition, analogous to similar axial pyridine bound cobaloximes<sup>29,33</sup>. The ligation between stilbene-derived pyridine motif and cobaloxime was definitively verified with the single crystal structure data of **C1**. As shown in **Figure 4**, the critical  $\text{N}^{\text{pyridine}}\text{-Co}$  bond distance was measured at 1.965 Å, similar to typical axial  $\text{N}^{\text{pyridine}}\text{-Co}$  bonds<sup>9</sup>. The aromatic rings along with the allylic group remained in the same plane in the hybrid complex **C1** that ensure an elongated conjugation in the stilbene moiety. The details of the crystal data collections and data refinement parameters are given in **Table 1**. The complete crystallographic information file (CIF) of the PS-catalyst hybrid complex was deposited in the Cambridge crystallographic data centre (CCDC No: 1883987)<sup>34</sup>.

A cyclic voltammetry (CV) experiment was performed with the PS-catalyst-hybrid complex **C1** starting with a cathodic scan in the range of 0.5 V to -1.8 V in DMF (**Figure 5**). An irreversible reduction signal was observed at -1.0 V (vs.  $\text{Fc}^{+/0}$ ) followed by two successive reversible signals at -1.3 and -1.5 V. The first reductive signal can be assigned as the metal based  $\text{Co(III/II)}$  reduction while the reversible signals were attributed to the stoichiometric redox processes at aromatic organic dye framework<sup>32</sup>. **C1** demonstrated a distinct catalytic signal at -1.25 V when water was added to the solution. Electrocatalytic  $\text{H}_2$  production was possibly responsible for this cathodic catalytic behavior. This hypothesis was corroborated by a gradual increase in that catalytic response following the addition of TFA in the same solution (**Figure 5**). The turnover frequency (TOF) for these catalytic responses was tabulated using the following equation:

$$\frac{i_{\text{cat}}}{i_p} = \frac{n}{0.4463} \left( \frac{RTk_{\text{obs}}}{Fv} \right)^{1/2} \quad (1)$$

where  $i_{\text{cat}}$  = catalytic current,  $i_p$  = stoichiometric current,  $n$  = number of electrons involved in this process,  $R$  = universal gas constant,  $T$  = temperature in K,  $F$  = 1 Faraday, and  $v$  = scan rate. The TOF for  $\text{H}_2$  production in the presence of water and aqueous TFA were  $30 \text{ s}^{-1}$  and  $172 \text{ s}^{-1}$ , respectively. The complementary chronocoulometric (bulk electrolysis) experiment was used along with the complementary gas chromatography (GC) to provide further evidence of  $\text{H}_2$

production during the catalytic step with 70% Faradaic efficiency (details in supplementary section, **Figure S1**).

The H<sub>2</sub> production activity of the cobaloxime core in **C1** was further investigated during the photo-catalytic studies. In this experiment, **C1** was loaded in an airtight container containing 30:70 water/DMF solvent along with TEOA sacrificial electron donor. This system was connected to the H<sub>2</sub> sensor and exposed to natural sunlight (power density ~ 100 mW/cm<sup>2</sup>) (**Figure 6**). As shown in **Figure 7**, the PS-catalyst hybrid complex **C1** displayed catalytic H<sub>2</sub> production immediately following the sunlight exposure. In this case, an almost linear increase in photocatalytic H<sub>2</sub> production was observed over time. The identity and purity of the photo-generated gas accumulated in the headspace of the set-up was validated by gas chromatography (GC). As illustrated in **Figure 8**, solar-driven, H<sub>2</sub> production was confirmed by the GC results. The minimal change in the comparative optical spectra demonstrated the stability of **C1** during this experiment (**Figure S2**).

#### FIGURE LEGENDS:

**Figure 1. Reaction scheme.** The scheme represents the synthetic route for the PS-catalyst hybrid complex.

**Figure 2. <sup>1</sup>H NMR spectra of PS-catalyst hybrid complex C1.** This figure displays the <sup>1</sup>H NMR of PS-catalyst hybrid complex recorded in d<sup>6</sup>-DMSO at room temperature. The aliphatic region consists of oxime-methyl groups (12 H, **a**), and PS-bound N-methyl groups (6 H, **b**) (black trace). The aromatic region consists of 10 H, containing both aromatic (**c**, **d**, **e**, **f**) and allylic (**g** and **h**) protons. The oxime (-NOH) protons are the most down-shielded protons (**i**) (red trace). The inset highlights the detailed splitting pattern of the aromatic (blue trace) and allylic protons (green trace).

**Figure 3. Comparative optical spectra.** The comparative Uv-vis spectra of PS (black trace), cobaloxime precursor (red trace), and PS-catalyst dyad **C1** (blue trace) recorded in DMF at room temperature. The formation of the hybrid complex distinctly red-shifted the LMCT band, while the  $\pi$ - $\pi^*$  transition remained same.

**Figure 4. Single crystal structure of photosensitizer-Cobaloxime hybrid C1.** ORTEP representation for **C1** with 50% thermal ellipsoids probability. The carbon (grey), hydrogen (white), oxygen (red), nitrogen (sky-blue), chlorine (green), and cobalt (deep blue) atoms are shown in the figures accordingly. One chloroform molecule was found inside the crystal lattice, but it is omitted here for clarity.

**Figure 5. Comparative cyclic voltammograms.** The comparative cyclic voltammograms (CVs) of 1 mM **C1** in only DMF (black trace), in the presence of 30:70 water/DMF (blue trace), and in the presence of 16 equivalent TFA in 30:70 water/DMF (red trace) were shown in the figure. The scans were performed in the presence of 0.1 M tetra-N-butyl ammonium fluoride (*n*-Bu<sub>4</sub>N<sup>+</sup>F<sup>-</sup>/TBAF) as supporting electrolyte utilizing 1mm glassy carbon disc working electrode, Ag/AgCl (in 1.0 M

AgNO<sub>3</sub>) reference electrode and platinum (Pt)-wire counter electrode at room temperature with 0.1 V/s scan rate. The initial scan direction is shown with the horizontal black arrow.

**Figure 6. The photocatalytic H<sub>2</sub> production monitoring system:** The schematic representation of the experimental set-up, consisting of an online H<sub>2</sub> detector, used for continuous monitoring H<sub>2</sub> production by photosensitizer-cobaloxime dyad **C1** under natural sunlight and complete aerobic condition.

**Figure 7. Photocatalytic H<sub>2</sub> production by C1 over time.** The accumulation of H<sub>2</sub> over time during the natural sunlight-driven photocatalysis by photosensitizer-cobaloxime hybrid complex **C1** as detected by the online H<sub>2</sub> detector.

**Figure 8. Comparative gas chromatography data.** Comparative gas chromatography (GC) data recorded for the head space gas collected from the photosensitizer-cobaloxime dyad **C1** placed under dark (black trace) and natural sunlight (blue trace). The red trace signified the signal from the 1% H<sub>2</sub> calibration gas mixture sample.

**Figure 9. Photocatalytic scheme for H<sub>2</sub> production by C1.** Possible photo-catalytic H<sub>2</sub> production cycle for the PS-catalyst hybrid complex **C1**. This mechanism presumably follows the sequence of excitation of the photosensitizer, transfer the excited electron to the catalyst via linker, and H<sub>2</sub> production catalysis at the reduced catalytic centre. The cationic photosensitizer returns to the ground state by accepting electron from the sacrificial electron donor.

## DISCUSSION:

The organic photosensitizer stilbene moiety was successfully incorporated into the cobaloxime core via the axial pyridine linkage (**Figure 1**). This strategy allowed us to devise a photosensitizer-cobaloxime hybrid complex **C1**. The presence of both the oxime and organic dye in the same molecular framework was evident from the single crystal structure of the **C1** (**Figure 4**). The phenyl and pyridine functionalities of the stilbene motif existed in the same plane via an elongated conjugation through the allylic group. The interaction between these variable groups of the organic dye continued even in the solution phase as corroborated by the <sup>1</sup>H NMR data (**Figure 2**). The stilbene molecule contained a dimethyl amine group that can exhibit a strong electron push via the conjugated aromatic-allylic network to the pyridine N-terminal<sup>32</sup>. This electronic interaction was expected to improve the σ-donation property of the N-pyridine towards the cobalt center in the axially coordinated Cobaloxime complex **C1**. The distinct alteration in the LMCT band of cobaloxime core along with red-shift of the π–π\* transition of the stilbene motif in **C1** indicated that the electronic interaction between the metal and photosensitizer modules (**Figure 3**).

The electrochemical data highlighted active H<sub>2</sub> production by this photosensitizer-cobaloxime hybrid **C1** in the presence of water (**Figure 5**). This data suggested that (a) the cobaloxime core in **C1** retained its intrinsic H<sub>2</sub> production activity even in the presence of organic dye in its periphery and (b) water can act as a proton source during the catalysis. These results led to the investigation of photocatalytic H<sub>2</sub> production by **C1**. During this experiment, an aqueous/DMF

solution of **C1**, containing a TEOA sacrificial electron donor, was exposed to natural sunlight under aerobic condition and the complete air-tight setup was connected with an online H<sub>2</sub> detector (**Figure 6**). A continuous accumulation of H<sub>2</sub> was noticed during this experiment without any lag period, highlighting the photo-driven H<sub>2</sub> production by **C1** (**Figure 7**). The production of H<sub>2</sub> during the photocatalytic conditions was further corroborated by the complementary GC experiments (**Figure 8**). This solar-driven H<sub>2</sub> production by **C1** possibly follows the typical catalytic cycle observed for cobaloxime-based photocatalytic devices that is illustrated in **Figure 9**<sup>21</sup>. Earlier studies by Eisenberg et al. also supported the proposed photocatalytic cycle<sup>35–37</sup>.

The experimental setup developed during this project can be utilized to screen a number of photocatalytic systems by varying the combinations of photosensitizers, catalysts, sacrificial electron donor, and the solution ingredients. There is a potential application of this system under broad reaction conditions as it is functional in the presence of natural sunlight. This simple setup can also be employed in couple with variable laser configurations for the in-depth analysis of the photocatalytic activity. Here, we have incorporated stilbene dye with the cobaloxime complex to generate moderate photocatalytic H<sub>2</sub> production hybrid. Their reactivity can be modified further by installing enzyme-inspired basic functionalities on the complex skeleton to further enhance the proton exchange rate, a critical step for the catalytic cycle<sup>38–40</sup>. This first generation photosensitizer-catalyst adduct provides an efficient, inexpensive, and green solar H<sub>2</sub> production pathway compared to the other existing H<sub>2</sub> generation techniques<sup>41</sup>. Hence, both the photocatalysts design strategy and solar-driven H<sub>2</sub> production detection technique will pave the way for the development of next generation photo-active assemblies to renovate the renewable energy circuit.

#### ACKNOWLEDGEMENTS:

Financial support was provided by IIT Gandhinagar and Government of India. We would also like to thank the extramural funding provided by Science and Engineering Research Board (SERB) (File no. EMR/2015/002462).

#### DISCLOSURE:

The authors have nothing to disclose.

#### REFERENCES:

1. Chu, S., Majumdar, A. Opportunities and challenges for a sustainable energy future. *Nature*. **488** (7411), 294–303 (2012).
2. Lewis, N.S., Nocera, D.G. Powering the planet: Chemical challenges in solar energy utilization. *Proceedings of the National Academy of Sciences of the United States of America*. **103** (43), 15729–15735 (2006).
3. Faunce, T.A. et al. Energy and environment policy case for a global project on artificial photosynthesis. *Energy and Environmental Science*. **6** (3), 695–698 (2013).
4. Artero, V., Fontecave, M. Solar fuels generation and molecular systems: is it homogeneous or heterogeneous catalysis? *Chemical Society Reviews*. **42** (6), 2338–2356 (2013).
5. Artero, V. Bioinspired catalytic materials for energy-relevant conversions. *Nature Energy*. **2**, 17131 (2017).



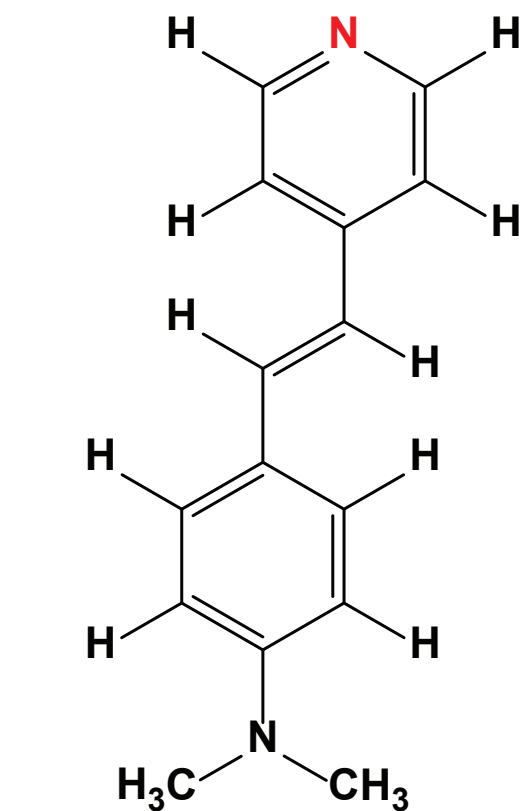
6. Ball, M., Wietschel, M. The future of hydrogen – opportunities and challenges. *International Journal of Hydrogen Energy*. **34** (2), 615–627 (2009).
7. da Silva Veras, T., Mozer, T.S., da Costa Rubim Messeder dos Santos, D., da Silva César, A. Hydrogen: Trends, production and characterization of the main process worldwide. *International Journal of Hydrogen Energy*. **42** (4), 2018–2033 (2017).
8. Artero, V., Fontecave, M. Some general principles for designing electrocatalysts with hydrogenase activity. *Coordination Chemistry Reviews*. **249** (15), 1518–1535 (2005).
9. Razavet, M., Artero, V., Fontecave, M. Proton Electroreduction Catalyzed by Cobaloximes: Functional Models for Hydrogenases. *Inorganic Chemistry*. **44** (13), 4786–4795 (2005).
10. Landrou, G., Panagiotopoulos, A.A., Ladomenou, K., Coutsolelos, A.G. Photochemical hydrogen evolution using Sn-porphyrin as photosensitizer and a series of Cobaloximes as catalysts. *Journal of Porphyrins and Phthalocyanines*. **20** (01n04), 534–541 (2016).
11. Panagiotopoulos, A., Ladomenou, K., Sun, D., Artero, V., Coutsolelos, A.G. Photochemical hydrogen production and cobaloximes: the influence of the cobalt axial N-ligand on the system stability. *Dalton Transactions*. **45** (15), 6732–6738 (2016).
12. Wakerley, D., Reisner, E. Development and understanding of cobaloxime activity through electrochemical molecular catalyst screening. *Physical Chemistry Chemical Physics*. **16** (12), 5739–5746 (2014).
13. Hawecker, J., Lehn, J.M., Ziessel, R. Efficient homogeneous photochemical hydrogen generation and water reduction mediated by cobaloxime or macrocyclic cobalt complexes. *Nouveau Journal de Chimie*. **7** (5), 271–277 (1983).
14. Du, P., Knowles, K., Eisenberg, R. A Homogeneous System for the Photogeneration of Hydrogen from Water Based on a Platinum(II) Terpyridyl Acetylide Chromophore and a Molecular Cobalt Catalyst. *Journal of the American Chemical Society*. **130** (38), 12576–12577 (2008).
15. Du, P., Schneider, J., Luo, G., Brennessel, W.W., Eisenberg, R. Visible Light-Driven Hydrogen Production from Aqueous Protons Catalyzed by Molecular Cobaloxime Catalysts. *Inorganic Chemistry*. **48** (11), 4952–4962 (2009).
16. To, W.-P. et al. Luminescent Organogold(III) Complexes with Long-Lived Triplet Excited States for Light-Induced Oxidative C-H Bond Functionalization and Hydrogen Production. *Angewandte Chemie International Edition*. **51** (11), 2654–2657 (2012).
17. Zhang, P. et al. Phosphine Coordination to a Cobalt Diimine–Dioxime Catalyst Increases Stability during Light-Driven H<sub>2</sub> Production. *Inorganic Chemistry*. **51** (4), 2115–2120 (2012).
18. McCormick, T.M. et al. Reductive Side of Water Splitting in Artificial Photosynthesis: New Homogeneous Photosystems of Great Activity and Mechanistic Insight. *Journal of the American Chemical Society*. **132** (44), 15480–15483 (2010).
19. Zhang, P. et al. Photocatalytic Hydrogen Production from Water by Noble-Metal-Free Molecular Catalyst Systems Containing Rose Bengal and the Cobaloximes of BF<sub>x</sub>-Bridged Oxime Ligands. *The Journal of Physical Chemistry C*. **114** (37), 15868–15874 (2010).
20. Dalle, K.E., Warnan, J., Leung, J.J., Reuillard, B., Karmel, I.S., Reisner, E. Electro- and Solar-Driven Fuel Synthesis with First Row Transition Metal Complexes. *Chemical Reviews*. **119** (4), 2752–2875 (2019).

21. Fihri, A., Artero, V., Razavet, M., Baffert, C., Leibl, W., Fontecave, M. Cobaloxime-Based Photocatalytic Devices for Hydrogen Production. *Angewandte Chemie International Edition*. **47** (3), 564–567 (2008).
22. Li, C., Wang, M., Pan, J., Zhang, P., Zhang, R., Sun, L. Photochemical hydrogen production catalyzed by polypyridyl ruthenium–cobaloxime heterobinuclear complexes with different bridges. *Journal of Organometallic Chemistry*. **694** (17), 2814–2819 (2009).
23. Mulfort, K.L., Tiede, D.M. Supramolecular Cobaloxime Assemblies for H<sub>2</sub> Photocatalysis: An Initial Solution State Structure–Function Analysis. *The Journal of Physical Chemistry B*. **114** (45), 14572–14581 (2010).
24. Zhang, P., Wang, M., Li, C., Li, X., Dong, J., Sun, L. Photochemical H<sub>2</sub> production with noble-metal-free molecular devices comprising a porphyrin photosensitizer and a cobaloxime catalyst. *Chemical Communications*. **46** (46), 8806–8808 (2009).
25. McCormick, T.M., Han, Z., Weinberg, D.J., Brennessel, W.W., Holland, P.L., Eisenberg, R. Impact of Ligand Exchange in Hydrogen Production from Cobaloxime-Containing Photocatalytic Systems. *Inorganic Chemistry*. **50** (21), 10660–10666 (2011).
26. S. Veldkamp, B., Han, W.-S., M. Dyar, S., W. Eaton, S., A. Ratner, M., R. Wasielewski, M. Photoinitiated multi-step charge separation and ultrafast charge transfer induced dissociation in a pyridyl -linked photosensitizer–cobaloxime assembly. *Energy & Environmental Science*. **6** (6), 1917–1928 (2013).
27. Roy, S., Bhunia, A., Schuth, N., Haumann, M., Ott, S. Light-driven hydrogen evolution catalyzed by a cobaloxime catalyst incorporated in a MIL-101(Cr) metal–organic framework. *Sustainable Energy & Fuels*. **2** (6), 1148–1152 (2018).
28. Song, T., Yu, J., Cui, Y., Yang, Y., Qian, G. Encapsulation of dyes in metal–organic frameworks and their tunable nonlinear optical properties. *Dalton Transactions*. **45** (10), 4218–4223 (2016).
29. Schrauzer, G.N., Parshall, G.W., Wonchoba, E.R. Bis(Dimethylglyoximate)Cobalt Complexes: (“Cobaloximes”). *Inorganic Syntheses*. 61–70 (2007).
30. Sheldrick, G.M. Sadabs, University of Gottingen, Germany Program for Empirical Absorption Correction of Area Detector Data (1996).
31. Gruene, T., Hahn, H.W., Luebben, A.V., Meilleur, F., Sheldrick, G.M. Refinement of macromolecular structures against neutron data with SHELXL2013. *Journal of Applied Crystallography*. **47** (Pt 1), 462–466 (2014).
32. Kumari, B., Paramasivam, M., Dutta, A., Kanvah, S. Emission and Color Tuning of Cyanostilbenes and White Light Emission. *ACS Omega*. **3** (12), 17376–17385 (2018).
33. Schrauzer, G.N., Lee, L.-P., Sibert, J.W. Alkylcobalamins and alkylcobaloximes. Electronic structure, spectra, and mechanism of photodealkylation. *Journal of the American Chemical Society*. **92** (10), 2997–3005 (1970).
34. Groom, C.R., Bruno, I.J., Lightfoot, M.P., Ward, S.C. The Cambridge Structural Database. *Acta Crystallographica Section B, Structural Science, Crystal Engineering and Materials*. **72** (Pt 2), 171–179 (2016).
35. Das, A., Han, Z., Haghighi, M.G., Eisenberg, R. Photogeneration of hydrogen from water using CdSe nanocrystals demonstrating the importance of surface exchange. *Proceedings of the National Academy of Sciences of the United States of America*. **110** (42), 16716–16723 (2013).

36. Das, A., Han, Z., Brennessel, W.W., Holland, P.L., Eisenberg, R. Nickel Complexes for Robust Light-Driven and Electrocatalytic Hydrogen Production from Water. *ACS Catalysis*. **5** (3), 1397–1406 (2015).
37. Eckenhoff, W.T., Eisenberg, R. Molecular systems for light driven hydrogen production. *Dalton Transactions*. **41** (42), 13004–13021 (2012).
38. Dutta, A., Appel, A.M., Shaw, W.J. Designing electrochemically reversible H<sub>2</sub> oxidation and production catalysts. *Nature Reviews Chemistry*. **2** (9), 244 (2018).
39. Savéant, J.-M. Proton Relays in Molecular Catalysis of Electrochemical Reactions: Origin and Limitations of the Boosting Effect. *Angewandte Chemie International Edition*. **58** (7), 2125–2128 (2019).
40. Khandelwal, S., Zamader, A., Nagayach, V., Dolui, D., Mir, A.Q., Dutta, A. Inclusion of Peripheral Basic Groups Activates Dormant Cobalt-Based Molecular Complexes for Catalytic H<sub>2</sub> Evolution in Water. *ACS Catalysis*. 2334–2344 (2019).
41. Staffell, I. et al. The role of hydrogen and fuel cells in the global energy system. *Energy & Environmental Science*. **12** (2), 463–491 (2019).

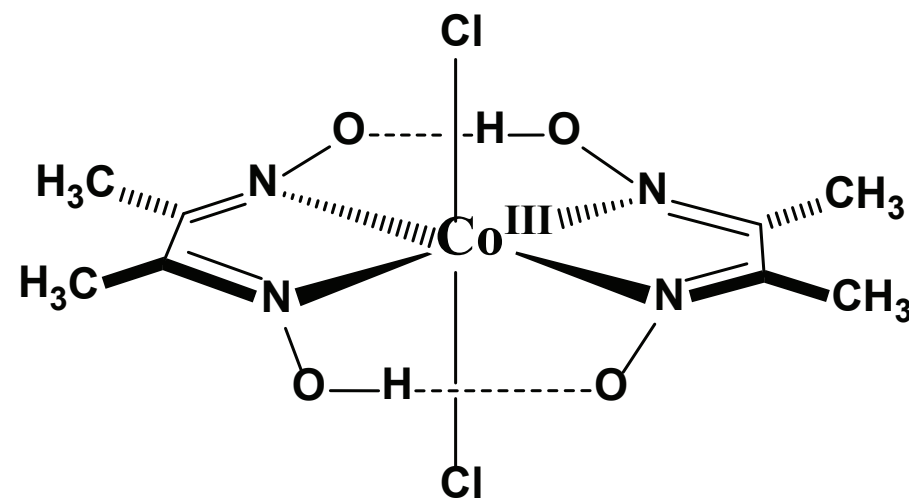
Figure 1

[Click here to access/download;Figure;Figure 1\\_scheme.ai](#) 

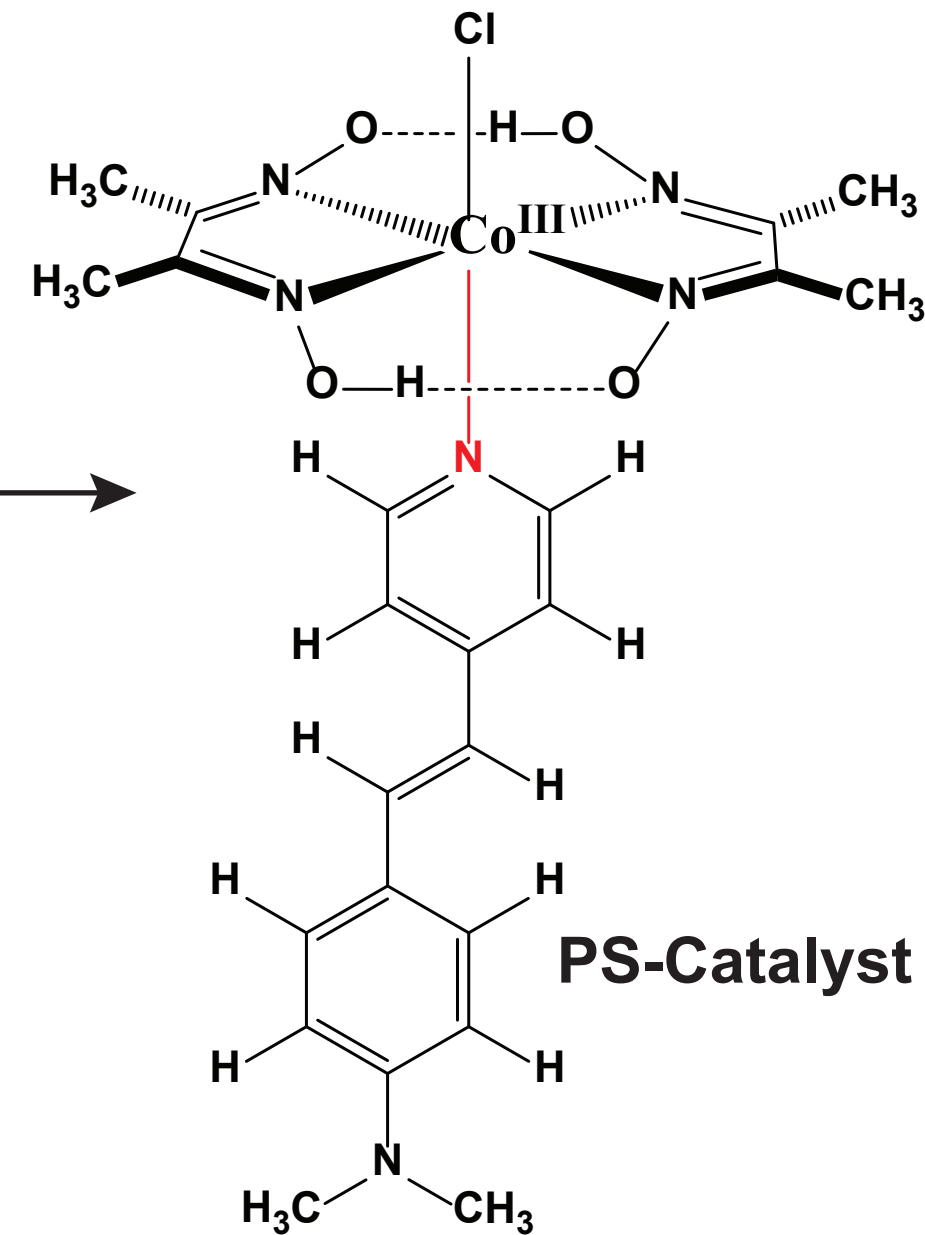


**Photosensitizer  
(PS)**

+



**Cobaloxime**



**PS-Catalyst hybrid**

Figure 2

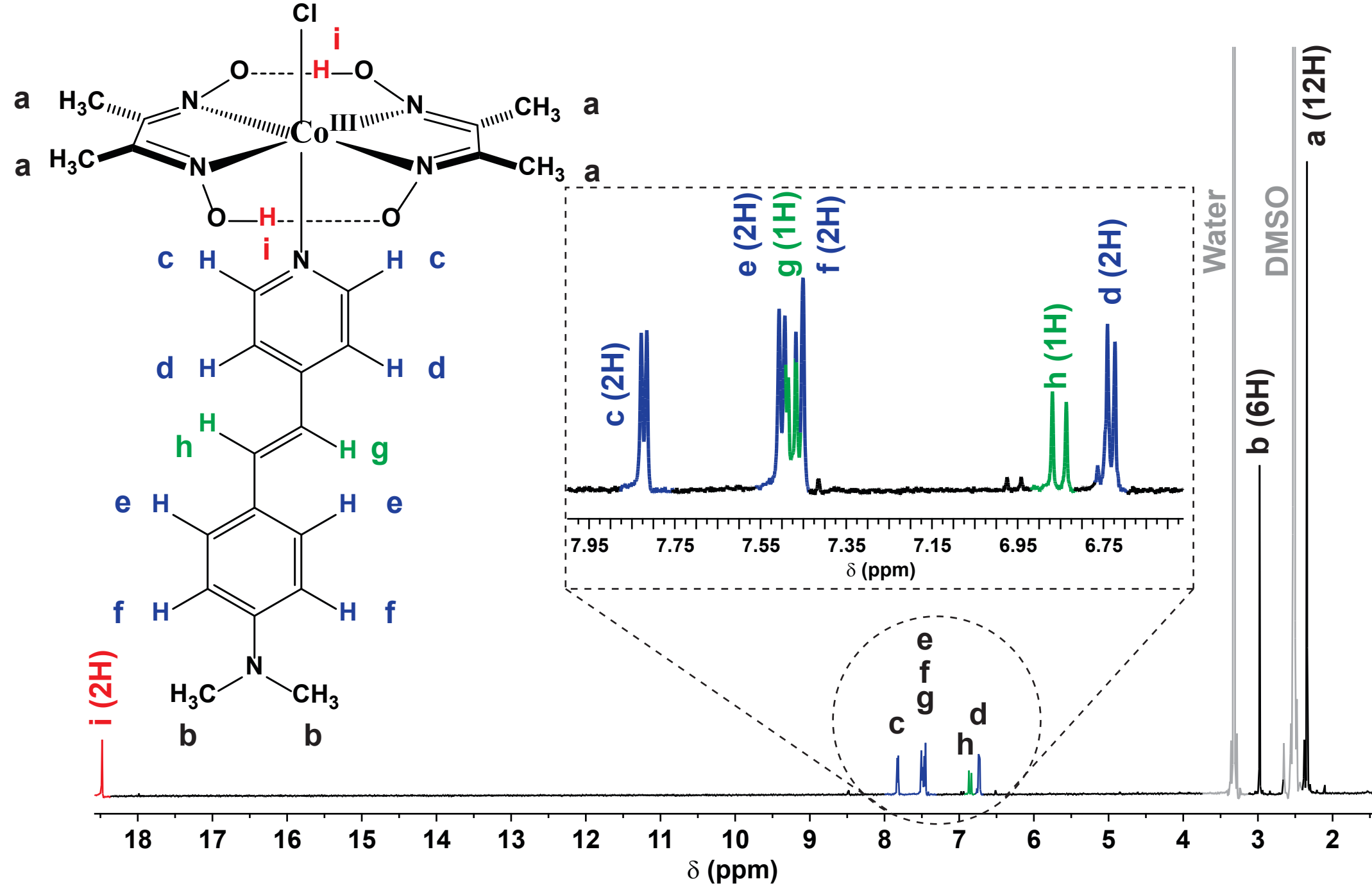
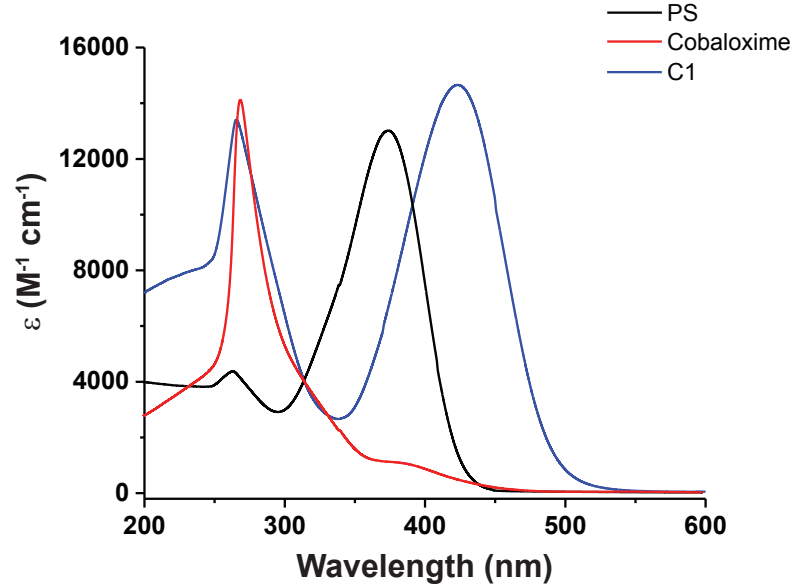
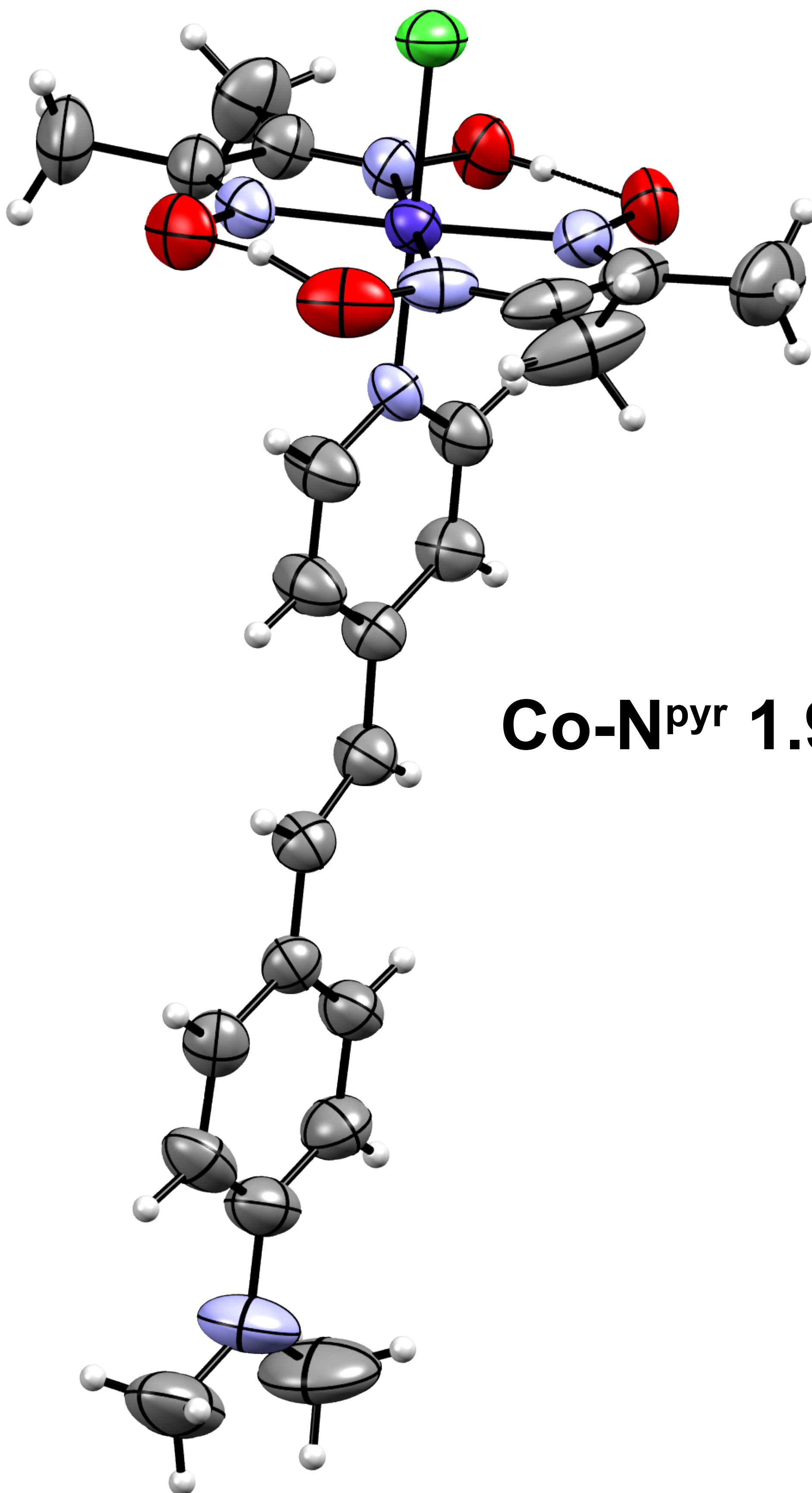


Figure 3





**Co-N<sub>pyr</sub> 1.965 Å**

Figure 5

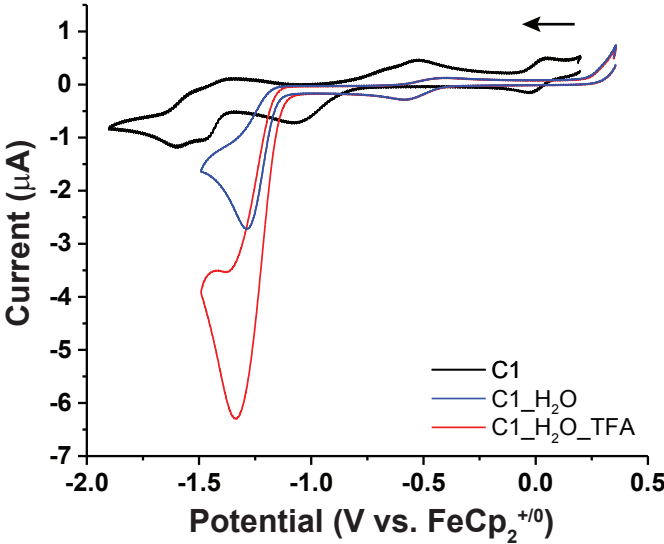
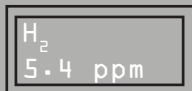




Figure 6



[Click here to access/download;Figure;Fig](#)



$H_2$  Detector

$H_2$  in  
head-  
space

PS-Cobaloxime  
Hybrid  
in Water/DMF

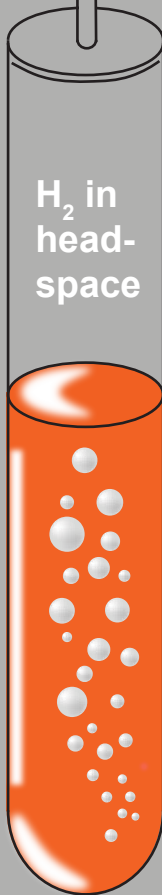
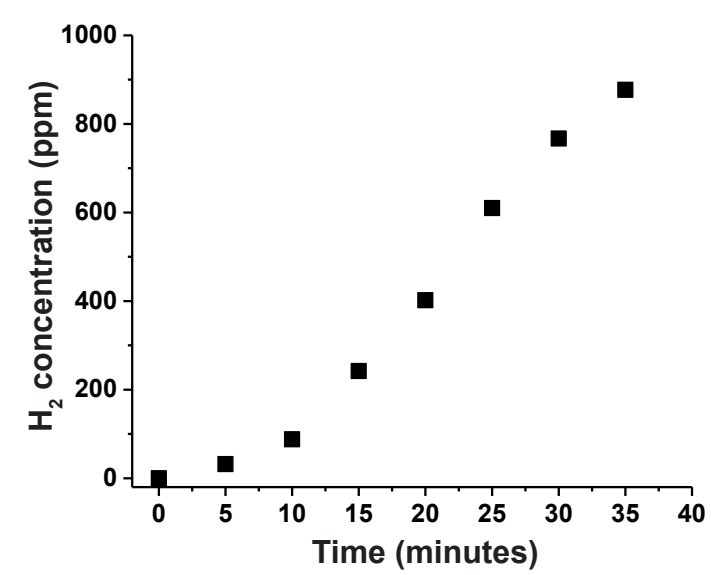


Figure 7

[Click here to access/download;Figure;Figure 7\\_H2 detection over time.ai](#) 



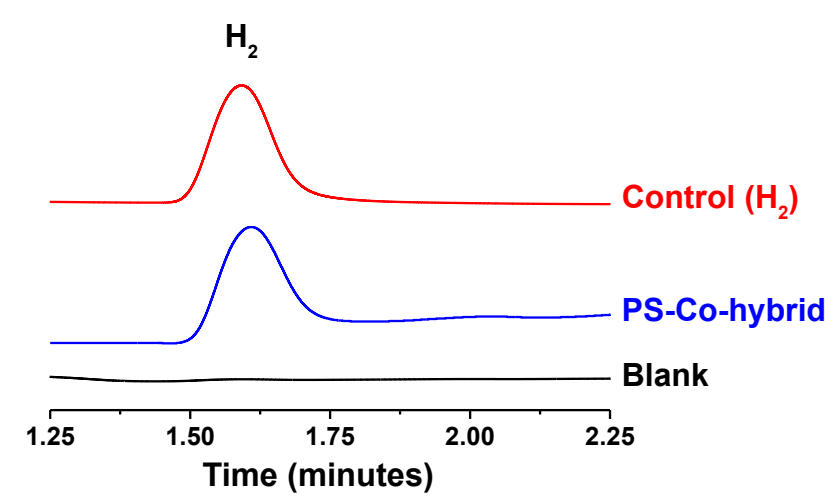
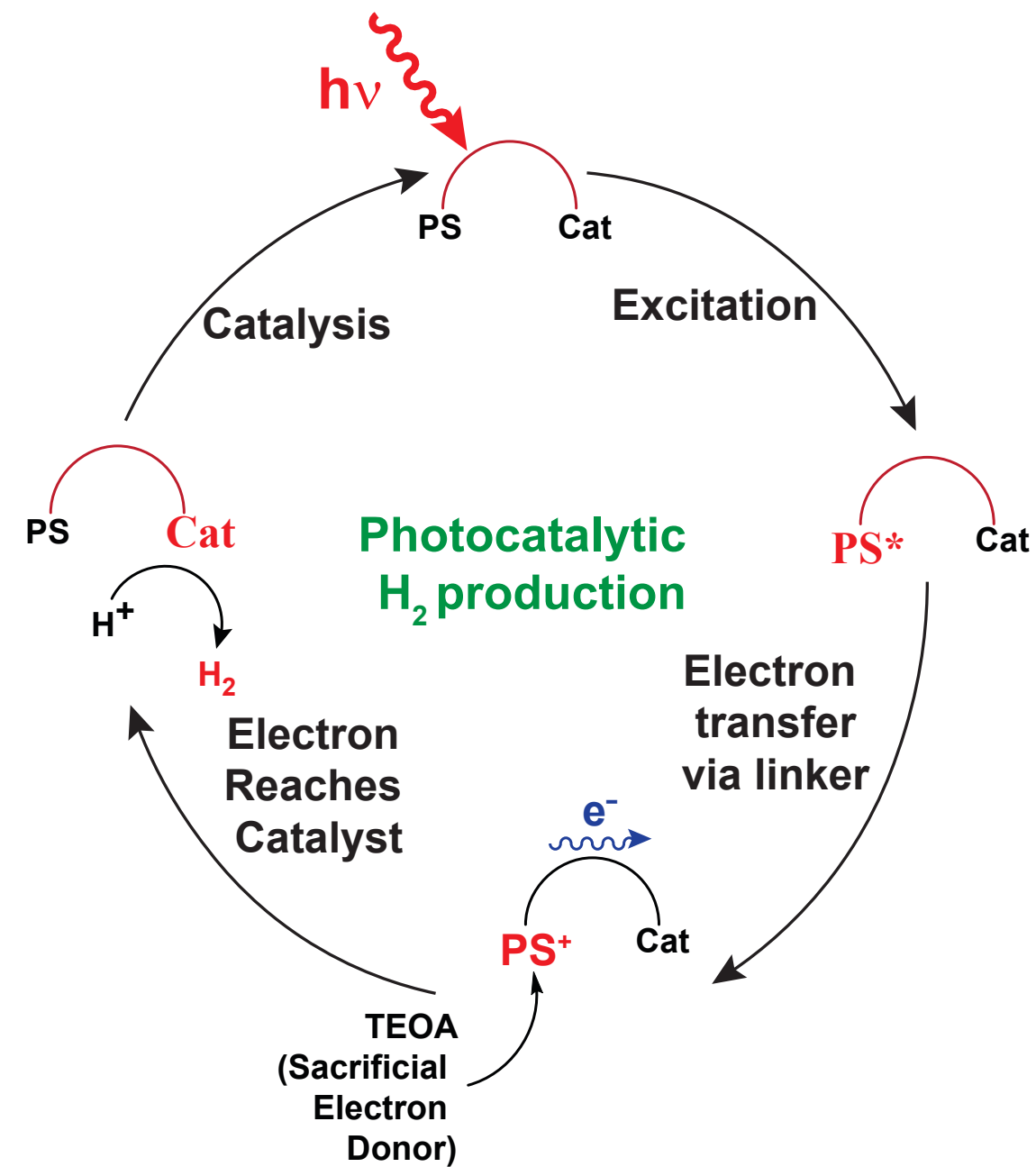


Figure 9



Name of Material/Equipment	Company	Catalog Number	Comments/Description
1 mm diameter glassy carbon disc electrode	ALS Co., Limited, Japan	2412	1
Acetone	SD fine chemicals	25214L10	27 mL
Ag/AgCl reference electrode	ALS Co., Limited, Japan	12171	1
Co(dm <sub>g</sub> ) <sub>2</sub> Cl <sub>2</sub>	Lab synthesised	NA	100 mg
CoCl <sub>2</sub> .6H <sub>2</sub> O	Sigma Aldrich	C2644	118 mg
d <sup>6</sup> dmso	Leonid Chemicals	D034EAS	650 µL
Deionized water from water purification system	NA	NA	500 mL
Dimethyl formamide	SRL Chemicals	93186	5 mL
Dimethyl glyoxime	Sigma Aldrich	40390	232 mg
Gas-tight syringe	SGE syringe Leur lock	21964	1
MES Buffer	Sigma	M8250	195 mg
Methanol	Finar	67-56-1	15 mL
Platinum counter electrode	ALS Co., Limited, Japan	2222	1
Stilbene Dye	Lab synthesised	NA	65 mg
TBAF(Tetra-n-butylammonium fluoride)	TCI Chemicals	T1338	20 mg
Triethanolamine	Finar	102-71-6	1 mL
Triethylamine	Sigma Aldrich	T0886	38 µL
Trifluoroacetic acid	Finar	76-05-1	10 µL
Whatman filter paper	GE Healthcare	1001125	2



1 Alewife Center #200  
Cambridge, MA 02140  
tel. 617.945.9051  
[www.jove.com](http://www.jove.com)

## ARTICLE AND VIDEO LICENSE AGREEMENT

Title of Article:	Developing photosensitizer-Cobaloxime hybrid for solar-driven H <sub>2</sub> production in aqueous aerobic conditions
Author(s):	Ab Qayoom Mir, Dependu Dolui, Shikha Khandelwal, Harshil Bhatt, Beena Kumari, Sanmitra Barman, Sriram Kanvah, Arnab Dutta

Item 1: The Author elects to have the Materials be made available (as described at <http://www.jove.com/publish>) via:

☒ Standard Access ☐ Open Access

Item 2: Please select one of the following items:

- ☒ The Author is **NOT** a United States government employee.
- ☐ The Author is a United States government employee and the Materials were prepared in the course of his or her duties as a United States government employee.
- ☐ The Author is a United States government employee but the Materials were NOT prepared in the course of his or her duties as a United States government employee.

### ARTICLE AND VIDEO LICENSE AGREEMENT

1. **Defined Terms.** As used in this Article and Video License Agreement, the following terms shall have the following meanings: **"Agreement"** means this Article and Video License Agreement; **"Article"** means the article specified on the last page of this Agreement, including any associated materials such as texts, figures, tables, artwork, abstracts, or summaries contained therein; **"Author"** means the author who is a signatory to this Agreement; **"Collective Work"** means a work, such as a periodical issue, anthology or encyclopedia, in which the Materials in their entirety in unmodified form, along with a number of other contributions, constituting separate and independent works in themselves, are assembled into a collective whole; **"CRC License"** means the Creative Commons Attribution-Non Commercial-No Derivs 3.0 Unported Agreement, the terms and conditions of which can be found at: <http://creativecommons.org/licenses/by-nc-nd/3.0/legalcode>; **"Derivative Work"** means a work based upon the Materials or upon the Materials and other pre-existing works, such as a translation, musical arrangement, dramatization, fictionalization, motion picture version, sound recording, art reproduction, abridgment, condensation, or any other form in which the Materials may be recast, transformed, or adapted; **"Institution"** means the institution, listed on the last page of this Agreement, by which the Author was employed at the time of the creation of the Materials; **"JoVE"** means MyJoVE Corporation, a Massachusetts corporation and the publisher of The Journal of Visualized Experiments; **"Materials"** means the Article and / or the Video; **"Parties"** means the Author and JoVE; **"Video"** means any video(s) made by the Author, alone or in conjunction with any other parties, or by JoVE or its affiliates or agents, individually or in collaboration with the Author or any other parties, incorporating all or any portion

of the Article, and in which the Author may or may not appear.

2. **Background.** The Author, who is the author of the Article, in order to ensure the dissemination and protection of the Article, desires to have the JoVE publish the Article and create and transmit videos based on the Article. In furtherance of such goals, the Parties desire to memorialize in this Agreement the respective rights of each Party in and to the Article and the Video.

3. **Grant of Rights in Article.** In consideration of JoVE agreeing to publish the Article, the Author hereby grants to JoVE, subject to **Sections 4** and **7** below, the exclusive, royalty-free, perpetual (for the full term of copyright in the Article, including any extensions thereto) license (a) to publish, reproduce, distribute, display and store the Article in all forms, formats and media whether now known or hereafter developed (including without limitation in print, digital and electronic form) throughout the world, (b) to translate the Article into other languages, create adaptations, summaries or extracts of the Article or other Derivative Works (including, without limitation, the Video) or Collective Works based on all or any portion of the Article and exercise all of the rights set forth in (a) above in such translations, adaptations, summaries, extracts, Derivative Works or Collective Works and (c) to license others to do any or all of the above. The foregoing rights may be exercised in all media and formats, whether now known or hereafter devised, and include the right to make such modifications as are technically necessary to exercise the rights in other media and formats. If the "Open Access" box has been checked in **Item 1** above, JoVE and the Author hereby grant to the public all such rights in the Article as provided in, but subject to all limitations and requirements set forth in, the CRC License.

## ARTICLE AND VIDEO LICENSE AGREEMENT

4. **Retention of Rights in Article.** Notwithstanding the exclusive license granted to JoVE in **Section 3** above, the Author shall, with respect to the Article, retain the non-exclusive right to use all or part of the Article for the non-commercial purpose of giving lectures, presentations or teaching classes, and to post a copy of the Article on the Institution's website or the Author's personal website, in each case provided that a link to the Article on the JoVE website is provided and notice of JoVE's copyright in the Article is included. All non-copyright intellectual property rights in and to the Article, such as patent rights, shall remain with the Author.

5. **Grant of Rights in Video – Standard Access.** This **Section 5** applies if the "Standard Access" box has been checked in **Item 1** above or if no box has been checked in **Item 1** above. In consideration of JoVE agreeing to produce, display or otherwise assist with the Video, the Author hereby acknowledges and agrees that, Subject to **Section 7** below, JoVE is and shall be the sole and exclusive owner of all rights of any nature, including, without limitation, all copyrights, in and to the Video. To the extent that, by law, the Author is deemed, now or at any time in the future, to have any rights of any nature in or to the Video, the Author hereby disclaims all such rights and transfers all such rights to JoVE.

6. **Grant of Rights in Video – Open Access.** This **Section 6** applies only if the "Open Access" box has been checked in **Item 1** above. In consideration of JoVE agreeing to produce, display or otherwise assist with the Video, the Author hereby grants to JoVE, subject to **Section 7** below, the exclusive, royalty-free, perpetual (for the full term of copyright in the Article, including any extensions thereto) license (a) to publish, reproduce, distribute, display and store the Video in all forms, formats and media whether now known or hereafter developed (including without limitation in print, digital and electronic form) throughout the world, (b) to translate the Video into other languages, create adaptations, summaries or extracts of the Video or other Derivative Works or Collective Works based on all or any portion of the Video and exercise all of the rights set forth in (a) above in such translations, adaptations, summaries, extracts, Derivative Works or Collective Works and (c) to license others to do any or all of the above. The foregoing rights may be exercised in all media and formats, whether now known or hereafter devised, and include the right to make such modifications as are technically necessary to exercise the rights in other media and formats. For any Video to which this **Section 6** is applicable, JoVE and the Author hereby grant to the public all such rights in the Video as provided in, but subject to all limitations and requirements set forth in, the CRC License.

7. **Government Employees.** If the Author is a United States government employee and the Article was prepared in the course of his or her duties as a United States government employee, as indicated in **Item 2** above, and any of the licenses or grants granted by the Author hereunder exceed the scope of the 17 U.S.C. 403, then the rights granted hereunder shall be limited to the maximum

rights permitted under such statute. In such case, all provisions contained herein that are not in conflict with such statute shall remain in full force and effect, and all provisions contained herein that do so conflict shall be deemed to be amended so as to provide to JoVE the maximum rights permissible within such statute.

8. **Protection of the Work.** The Author(s) authorize JoVE to take steps in the Author(s) name and on their behalf if JoVE believes some third party could be infringing or might infringe the copyright of either the Author's Article and/or Video.

9. **Likeness, Privacy, Personality.** The Author hereby grants JoVE the right to use the Author's name, voice, likeness, picture, photograph, image, biography and performance in any way, commercial or otherwise, in connection with the Materials and the sale, promotion and distribution thereof. The Author hereby waives any and all rights he or she may have, relating to his or her appearance in the Video or otherwise relating to the Materials, under all applicable privacy, likeness, personality or similar laws.

10. **Author Warranties.** The Author represents and warrants that the Article is original, that it has not been published, that the copyright interest is owned by the Author (or, if more than one author is listed at the beginning of this Agreement, by such authors collectively) and has not been assigned, licensed, or otherwise transferred to any other party. The Author represents and warrants that the author(s) listed at the top of this Agreement are the only authors of the Materials. If more than one author is listed at the top of this Agreement and if any such author has not entered into a separate Article and Video License Agreement with JoVE relating to the Materials, the Author represents and warrants that the Author has been authorized by each of the other such authors to execute this Agreement on his or her behalf and to bind him or her with respect to the terms of this Agreement as if each of them had been a party hereto as an Author. The Author warrants that the use, reproduction, distribution, public or private performance or display, and/or modification of all or any portion of the Materials does not and will not violate, infringe and/or misappropriate the patent, trademark, intellectual property or other rights of any third party. The Author represents and warrants that it has and will continue to comply with all government, institutional and other regulations, including, without limitation all institutional, laboratory, hospital, ethical, human and animal treatment, privacy, and all other rules, regulations, laws, procedures or guidelines, applicable to the Materials, and that all research involving human and animal subjects has been approved by the Author's relevant institutional review board.

11. **JoVE Discretion.** If the Author requests the assistance of JoVE in producing the Video in the Author's facility, the Author shall ensure that the presence of JoVE employees, agents or independent contractors is in accordance with the relevant regulations of the Author's institution. If more than one author is listed at the beginning of this Agreement, JoVE may, in its sole

## ARTICLE AND VIDEO LICENSE AGREEMENT

discretion, elect not take any action with respect to the Article until such time as it has received complete, executed Article and Video License Agreements from each such author. JoVE reserves the right, in its absolute and sole discretion and without giving any reason therefore, to accept or decline any work submitted to JoVE. JoVE and its employees, agents and independent contractors shall have full, unfettered access to the facilities of the Author or of the Author's institution as necessary to make the Video, whether actually published or not. JoVE has sole discretion as to the method of making and publishing the Materials, including, without limitation, to all decisions regarding editing, lighting, filming, timing of publication, if any, length, quality, content and the like.

12. **Indemnification.** The Author agrees to indemnify JoVE and/or its successors and assigns from and against any and all claims, costs, and expenses, including attorney's fees, arising out of any breach of any warranty or other representations contained herein. The Author further agrees to indemnify and hold harmless JoVE from and against any and all claims, costs, and expenses, including attorney's fees, resulting from the breach by the Author of any representation or warranty contained herein or from allegations or instances of violation of intellectual property rights, damage to the Author's or the Author's institution's facilities, fraud, libel, defamation, research, equipment, experiments, property damage, personal injury, violations of institutional, laboratory, hospital, ethical, human and animal treatment, privacy or other rules, regulations, laws, procedures or guidelines, liabilities and other losses or damages related in any way to the submission of work to JoVE, making of videos by JoVE, or publication in JoVE or elsewhere by JoVE. The Author shall be responsible for, and shall hold JoVE harmless from, damages caused by lack of sterilization, lack of cleanliness or by contamination due to

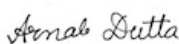
the making of a video by JoVE its employees, agents or independent contractors. All sterilization, cleanliness or decontamination procedures shall be solely the responsibility of the Author and shall be undertaken at the Author's expense. All indemnifications provided herein shall include JoVE's attorney's fees and costs related to said losses or damages. Such indemnification and holding harmless shall include such losses or damages incurred by, or in connection with, acts or omissions of JoVE, its employees, agents or independent contractors.

13. **Fees.** To cover the cost incurred for publication, JoVE must receive payment before production and publication of the Materials. Payment is due in 21 days of invoice. Should the Materials not be published due to an editorial or production decision, these funds will be returned to the Author. Withdrawal by the Author of any submitted Materials after final peer review approval will result in a US\$1,200 fee to cover pre-production expenses incurred by JoVE. If payment is not received by the completion of filming, production and publication of the Materials will be suspended until payment is received.

14. **Transfer, Governing Law.** This Agreement may be assigned by JoVE and shall inure to the benefits of any of JoVE's successors and assignees. This Agreement shall be governed and construed by the internal laws of the Commonwealth of Massachusetts without giving effect to any conflict of law provision thereunder. This Agreement may be executed in counterparts, each of which shall be deemed an original, but all of which together shall be deemed to be one and the same agreement. A signed copy of this Agreement delivered by facsimile, e-mail or other means of electronic transmission shall be deemed to have the same legal effect as delivery of an original signed copy of this Agreement.

A signed copy of this document must be sent with all new submissions. Only one Agreement is required per submission.

### CORRESPONDING AUTHOR

Name:	Arnab Dutta	
Department:	Chemistry	
Institution:	Indian Institute of Technology Gandhinagar	
Title:	Assistant Professor	
Signature:		Date: 6th May, 2019

Please submit a **signed** and **dated** copy of this license by one of the following three methods:

1. Upload an electronic version on the JoVE submission site
2. Fax the document to +1.866.381.2236
3. Mail the document to JoVE / Attn: JoVE Editorial / 1 Alewife Center #200 / Cambridge, MA 02140



To

Phillip Steindel, Ph.D.

Review Editor,

JoVE.

Dear Editor,

We thank you and the reviewers for the invaluable comments/suggestions on our submitted manuscript titled “Developing photosensitizer-Cobaloxime hybrid for solar-driven H<sub>2</sub> production in aqueous aerobic conditions”. We have now modified our manuscript as per the editorial comments. We have provided our point by point response to each of the point as following.

Yours’ Sincerely,

Arnab Dutta

---

#### Editorial and production comments:

1. We need a title card at the beginning of the video that contains, at the very least, the title of the article. Most of our videos also include the authors' names and affiliations on that title card.

**Response:** *Now, we have added a title card accordingly.*

2. 4.3.3 (manuscript)/3:10(video): This is still 2 hours in the manuscript and 3 hours in the video.

**Response:** *Now, we have rectified this discrepancy accordingly.*

3. Figure 2 legend: This is still a bit confusing-isn't g an allylic hydrogen too?

**Response:** *Now, we have changed the Figure 2 legend accordingly.*

4. Figure 4 (including in video, 5:43-6:06): please use ‘Å’ instead of A<sup>0</sup>

**Response:** *Now, we have altered the expression of Å accordingly.*

## Supplementary Information

### Developing photosensitizer-Cobaloxime hybrid for solar-driven H<sub>2</sub> production in aqueous aerobic conditions

Ab Qayoom Mir<sup>1</sup>, Dependu Dolui<sup>1</sup>, Shikha Khandelwal<sup>1</sup>, Harshil Bhatt<sup>2</sup>, Beena Kumari<sup>1</sup>,  
Sanmitra Barman<sup>3</sup>, Sriram Kanvah<sup>1</sup>, Arnab Dutta<sup>1\*</sup>

<sup>[1]</sup> Chemistry Discipline, Indian Institute of Technology Gandhinagar, Gujarat 382355, India

<sup>[2]</sup> Chemistry Department, Uka Tarsadia University, Bardoli, Gujarat 394350, India

<sup>[3]</sup> Applied Sciences Department, BML Munjal University, Haryana 122413, India

## Bulk Electrolysis or chronocoulometric experiment

The chronocoulometric experiment for complex C1 was executed in a four-neck glass vessel (Volume 150 mL including the head space) where a coiled 23 cm Pt wire (counter electrode), Ag/AgCl (in 1.0 M AgNO<sub>3</sub> as reference electrode), and reticulated vitreous carbon (working electrode) was inserted in three of those necks. The last of the necks was closed with a 14/20 rubber septum, which was used for N<sub>2</sub> purging before the experiment and for headspace gas collection (via gas tight leur-lock syringe). During the experiment, 75 mL of 0.20 mM C1 was included in the vessel along with all the electrodes and a magnetic bead in a gas-tight manner. After that, the solution was purged with N<sub>2</sub> for one hour. Then, the purging was stopped, and the chrono-coulometric experiment was started at -1.3 V vs. ferrocene couple in 30:70 water/DMF. The solution was continuously stirred at 500 rpm with a magnetic stirrer during the experiment. The headspace gas was collected by a gas-tight leur-lock syringe after 30 minutes to analyze via a gas chromatography (GC) instrument. The GC was calibrated with a control gas mixture (49.5% H<sub>2</sub> in N<sub>2</sub>).

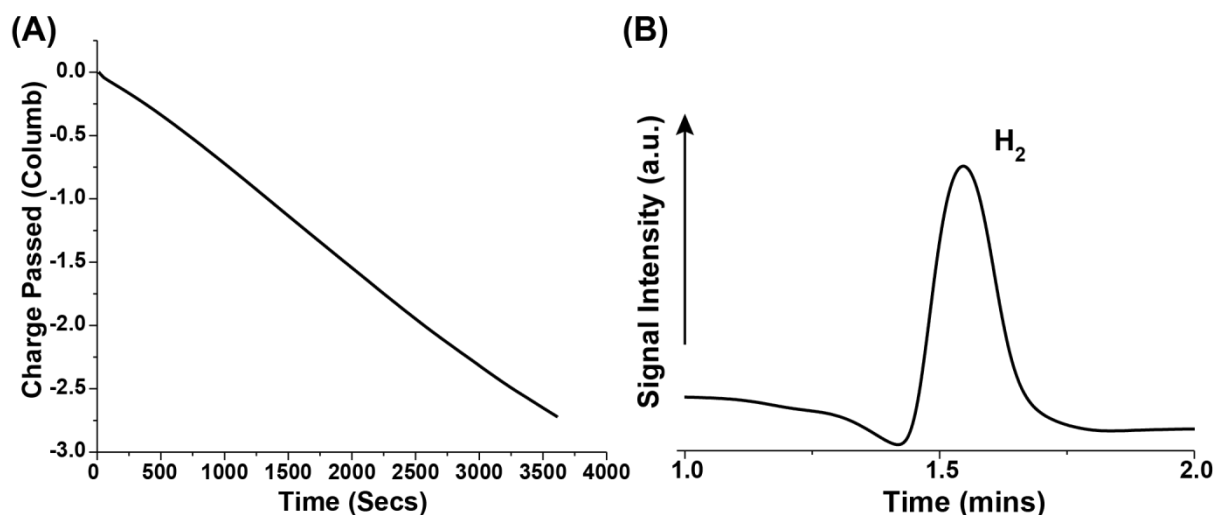


Figure S1. (A) The charge passed during the chronocoulometric experiment performed with 0.20 mM C1 in 30:70 water: acetonitrile media after 1 hour of electrolysis at -1.3 V vs. ferrocene couple. (B) The gas chromatography trace of the headspace gas following the bulk electrolysis experiment demonstrated the formation of H<sub>2</sub> during the experiment.

## Calculation of Faradic efficiency during chronocoulometric experiment

$$\text{Overall charge passed for catalytic HER} = 3.62 \text{ C}$$

$$\text{Amount of H}_2 \text{ expected} = \frac{3.62 \text{ C}}{96485 \times 2 \text{ C}} \text{ mol} = 18.75 \mu\text{mol} = \left(0.224 \frac{\text{mL}}{\mu\text{mol}} \times 18.75 \text{ mmol}\right) = 4.2 \text{ mL}$$

$$\text{Amount of H}_2 \text{ detected in headspace by GC} = 2.9 \text{ mL (calibrated by control)}$$

$$\% \text{ of current efficiency of C1 bulk electrolysis} = \frac{2.9}{4.2} \% = 69\%$$

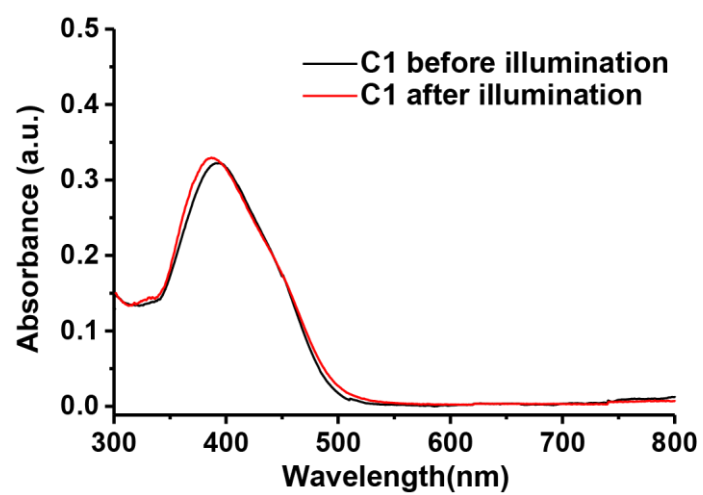


Figure S2. The comparative optical spectra recorded for C1 before (black trace) and after the illumination (red trace) exhibiting the stability of the complex during the experiment.

**Table 1. Crystallographic important parameters for C1.**

Crystal Data	
CCDC Number	1883987
Moiety formula	C1.(CHCl <sub>3</sub> )
Empirical formula	C <sub>23</sub> H <sub>30</sub> ClCoN <sub>6</sub> O <sub>4</sub> . (CHCl <sub>3</sub> )
Formula weight	668.28
Crystal Size (mm <sup>3</sup> )	0.348 x 0.179 x 0.051
Crystal Habit	Red Cubic
Temperature (K)	297.31
Radiation	MoK <sub>α</sub> (λ=0.71073)
Crystal system	Triclinic
Space group	P-1
Unit cell dimensions	11.345 (3)
a/b/c Å	12.534 (3)
	13.244 (3)
Unit cell angles	64.215 (6)
α/β/ γ (°)	68.735 (4)
	89.672 (5)
Unit cell volume (Å <sup>3</sup> )	1554.2 (6)
Z	2
Calculated density (g/cm <sup>3</sup> )	1.428
Absorption coefficient (mm <sup>-1</sup> )	0.935
F (000)	688.0
Θ range for all data collection (°)	5.834 to 55.862
Index ranges	-14 < h < 14
	-16 < k < 16
	-17 < l < 17

Reflections collected	38751
Independent reflections	7396 [ $R_{\text{int}} = 0.0816$ , $R_{\text{sigma}} = 0.0625$ ]
Data/restraints/parameters	7396/0/366
Completeness to $\theta_{\text{max}}$	0.993
<b>Refinement statistics</b>	
Final R indices [ $>2\sigma(I)$ ]	$R_1 = 0.0754$ , $wR_2 = 0.2109$
R indices (all data)	$R_1 = 0.1143$ , $wR_2 = 0.2392$
Goodness-of-fit on $F^2$	1.451

**Table 2. Bond Lengths for C1(CHCl<sub>3</sub>).**

Atom	Atom	Length/Å	Atom	Atom	Length/Å
Co <sup>(1)</sup>	Cl <sup>(1)</sup>	2.2342(11)	C <sup>(3)</sup>	C <sup>(4)</sup>	1.497(7)
Co <sup>(1)</sup>	N <sup>(1)</sup>	1.884(3)	C <sup>(5)</sup>	C <sup>(6)</sup>	1.491(6)
Co <sup>(1)</sup>	N <sup>(2)</sup>	1.898(3)	C <sup>(6)</sup>	C <sup>(7)</sup>	1.457(6)
Co <sup>(1)</sup>	N <sup>(3)</sup>	1.896(3)	C <sup>(7)</sup>	C <sup>(8)</sup>	1.492(6)
Co <sup>(1)</sup>	N <sup>(4)</sup>	1.885(3)	C <sup>(9)</sup>	C <sup>(10)</sup>	1.366(5)
Co <sup>(1)</sup>	N <sup>(5)</sup>	1.965(3)	C <sup>(10)</sup>	C <sup>(11)</sup>	1.388(5)
O <sup>(1)</sup>	N <sup>(1)</sup>	1.334(4)	C <sup>(11)</sup>	C <sup>(12)</sup>	1.397(6)
O <sup>(2)</sup>	N <sup>(2)</sup>	1.348(5)	C <sup>(11)</sup>	C <sup>(14)</sup>	1.453(5)
O <sup>(3)</sup>	N <sup>(3)</sup>	1.353(5)	C <sup>(12)</sup>	C <sup>(13)</sup>	1.350(6)
O <sup>(4)</sup>	N <sup>(4)</sup>	1.335(4)	C <sup>(14)</sup>	C <sup>(15)</sup>	1.313(5)
N <sup>(1)</sup>	C <sup>(6)</sup>	1.293(5)	C <sup>(15)</sup>	C <sup>(16)</sup>	1.442(5)
N <sup>(2)</sup>	C <sup>(2)</sup>	1.282(6)	C <sup>(16)</sup>	C <sup>(17)</sup>	1.390(6)
N <sup>(3)</sup>	C <sup>(3)</sup>	1.277(5)	C <sup>(16)</sup>	C <sup>(21)</sup>	1.398(5)
N <sup>(4)</sup>	C <sup>(7)</sup>	1.278(5)	C <sup>(17)</sup>	C <sup>(18)</sup>	1.374(6)
N <sup>(5)</sup>	C <sup>(9)</sup>	1.343(5)	C <sup>(18)</sup>	C <sup>(19)</sup>	1.397(6)
N <sup>(5)</sup>	C <sup>(13)</sup>	1.332(5)	C <sup>(19)</sup>	C <sup>(20)</sup>	1.403(7)
N <sup>(6)</sup>	C <sup>(19)</sup>	1.368(6)	C <sup>(20)</sup>	C <sup>(21)</sup>	1.368(6)
N <sup>(6)</sup>	C <sup>(22)</sup>	1.489(9)	Cl <sup>(15)</sup>	C <sup>(15)</sup>	1.690(9)
N <sup>(6)</sup>	C <sup>(23)</sup>	1.379(8)	Cl <sup>(25)</sup>	C <sup>(15)</sup>	1.666(8)
C <sup>(1)</sup>	C <sup>(2)</sup>	1.503(6)	Cl <sup>(35)</sup>	C <sup>(15)</sup>	1.657(8)
C <sup>(2)</sup>	C <sup>(3)</sup>	1.465(7)			